THE ASTROPHYSICAL JOURNAL, 195:157–174, 1975 January 1

RADIATION-DRIVEN WINDS IN Of STARS

JOHN I. CASTOR,* DAVID C. ABBOTT, AND RICHARD I. KLEIN
Joint Institute for Laboratory Astrophysics, University of Colorado and National Bureau of Standards
Received 1974 June 6

ABSTRACT

The large number of subordinate lines of a representative ion are found to have a dominant effect on the force of radiation on material in O star atmospheres. The force is increased over that due to resonance lines alone so that rates of mass loss are obtained which are 100 times greater than previously thought possible. The force is related to the solution of the line-transfer problem, and it becomes a function of the local velocity gradient. A new stellar wind theory, with a different interpretation of the singular point, is developed to treat this situation. The rate of mass loss, and other properties of the model, are uniquely specified by the luminosity, mass, and radius of the star. Alternative static models do not exist. Numerical results give a rate of mass loss $6 \times 10^{-6}\,\mathfrak{M}_\odot$ per year for an O5 star, with a terminal velocity of 1500 km s^{-1}. The rate of mass loss is sensitive to stellar parameters, while the terminal velocity is not. The continuum optical depth in the expanding envelope is about 0.16, of the right order to explain the reduced brightness temperature observed in ζ Pup. There is sufficient mass in the envelope for recombination to produce the emission lines of H and of He II which are observed, with approximately the proper strength. The rate of mass loss corresponds to a loss of more than 25 percent of the star's mass during main-sequence hydrogen burning, with obvious consequences for stellar evolution, and with the possibility of modified surface abundances.

Subject headings: atmospheres, stellar — mass loss — Of-type stars — stellar winds

I. INTRODUCTION

In a previous paper one of the authors has discussed approximations for the force exerted on the stellar material as a result of the absorption and scattering of line radiation (Castor 1974*a*, referred to below as Paper I). This force is thought (see, for example, the review by Mihalas 1974) to be responsible for the outflow of material in Of and perhaps Wolf-Rayet stars. In this paper we combine the force approximations with a large tabulation of oscillator strengths for C III (Castor 1974*c*) to produce a realistic quantitative model for an Of star. In the process we show that a great number of lines make important contributions to the total force, so that the force due to the resonance lines alone is relatively unimportant. For this reason the rates of mass loss we predict are about 100 times as great as the predictions of Lucy and Solomon (1970), who used essentially the same model but took only resonance lines into account. The larger rates of mass loss improve the agreement with observation for the continuous spectrum and also for the intensities of the emission lines. The mass loss during the main-sequence phase of evolution also becomes large enough to possibly affect the course of evolution.

The approximation we introduce for the force due to the lines is a function of the local velocity gradient. For this reason the usual theory of the solar wind (cf. Parker 1960; Brandt 1970) is no longer applicable; the derivative of the velocity is now defined in terms of the radius and velocity as the solution of a nonlinear equation. We describe the properties of the regular singular points of such an equation and find the relations that generalize the conditions for regularity at the sonic point. Just as in the solar wind theory (if the energy deposition, if any, is specified), the rate of mass loss is an eigenvalue that is determined by giving the luminosity, the mass, and a reference radius of the star.

The solution of the equation of motion that is found is characterized in the supersonic region by an almost constant value of the ratio of the acceleration of the flow to the acceleration of gravity, a ratio of about 1.5. This means that the velocity could be approximated in this region by the simple function $v = v_\infty(1 - r_s/r)^{1/2}$ which has frequently been used, with little justification, for line profile calculations (see Chandrasekhar 1934; Castor 1970; Van Blerkom 1973). The terminal velocity v_∞ also must be slightly more than the escape velocity, in agreement with the displacements of UV resonance lines.

The actual run of density with radius calculated for this model has been used in the LTE model atmosphere code described by Castor (1974*b*) to predict the emergent continuous spectrum. Surprisingly, the energy distribution is found to be essentially identical with that of a hydrostatic equilibrium model, a circumstance that is attributed to there being no creation of continuum photons in the extended electron-scattering envelope. This is consistent with the ground-based spectrophotometry of ζ Pup, for which the energy distribution is in exact agreement with the hydrostatic equilibrium, plane-parallel non–LTE model atmosphere of Mihalas (1972) with the parameters $T_{\rm eff} = 50{,}000°$ K and $\log g = 4$ if the star is assumed to have the average reddening of nine B stars in the field. The large flux deficiency of ζ Pup in the ultraviolet is then attributed to the enhanced line blanketing produced

* Also Department of Physics and Astrophysics, University of Colorado.

by the outflowing material. One respect in which the radiation fields of the flow model and the hydrostatic model do differ is in the size of the apparent emitting surface: it is larger in the flow model, which has an extended scattering envelope. This is sufficient to explain the low surface brightness found by Davis *et al.* (1970). Rough estimates of the intensity of the emission at Hα and at λ4686 give agreement with observations for several of the more extreme Of stars.

These points are all elaborated in the remainder of this paper. Section II deals with the calculation of the force produced by an ensemble of C III lines, how this is used to represent the total force on the material, and introduces a fitting-formula for the force. Section III develops the theory for a stellar wind that is driven by this force. Section IV gives the numerical results for an O5f model computed using the theory of § III. The model atmosphere calculation based on the model of § IV is discussed in § V. Some conclusions and a preview of further work occupy § VI.

II. THE AGGREGATE RADIATION FORCE PRODUCED BY THE C III SPECTRUM

In Paper I it was shown that in both static and rapidly expanding atmospheres the force due to an optically thick line is proportional to the line strength but inversely proportional, approximately, to the line optical depth, and therefore independent of the line strength overall. It is well known that for the prevalent ion of an abundant element such as C, N, or O there are a large number of lines that are optically thick over most of the atmosphere of a hot star. We now find that they all contribute equally to the force, or, to be more accurate, in proportion to the continuum flux at their respective frequencies. It therefore becomes essential to use a list of lines for the force computation which is as complete as possible. While such lists can readily be constructed using the term tables (Moore 1949), to obtain a comparable list of reliable oscillator strengths is another matter entirely. In connection with another problem a large list of oscillator strengths of fair accuracy has been computed for the ion C III (Castor 1974*c*). This list includes all the transitions among the first 80 or so terms of the ion, and numbers about 900 multiplets. (The lines of any multiplet will be treated as a single line for this work.) The uncertainty of most of the oscillator strengths is probably about 25 percent, which is sufficient for our purpose.

For the force due to a single line we take the approximate result of Paper I, so that the force contributed by the line, per unit mass of material, is given by

$$f_{\mathrm{rad},L} = \frac{\kappa_L F_c \Delta\nu_D}{c} \min\,(1, 1/\tau_L)\,, \tag{1}$$

where κ_L is the monochromatic line absorption coefficient, per unit mass, divided by the line profile function; that function is assumed to be normalized on a scale of frequency expressed in thermal Doppler units. The line optical depth τ_L differs in the static and expanding cases: in the static atmosphere it is given by

$$\tau_L = \int_r^\infty \kappa_L \rho dr\,; \tag{2}$$

and in the expanding atmosphere by

$$\tau_L = \kappa_L \rho v_{\mathrm{th}} \left|\frac{dv}{dr}\right|^{-1}. \tag{3}$$

(In the static atmosphere τ_L measures the total column density of absorbers; in the expanding atmosphere τ_L counts only the absorbers in a section of the column across which the velocity changes by v_{th}, the random velocity of the atoms.) We introduce the ratio β of the mass scattering coefficient of the free electrons, σ_e, to the line opacity κ_L (σ_e is a number of the order of 0.4 cm^2 g^{-1}). We introduce an optical depth variable which is independent of the line strength,

$$t = \beta\tau_L\,, \tag{4}$$

so that, in view of equations (2) and (3), we have

$$t = \int_r^\infty \sigma_e \rho dr \qquad \text{(static)}$$

$$= \sigma_e \rho v_{\mathrm{th}} \left|\frac{dv}{dr}\right|^{-1} \qquad \text{(expanding)}\,. \tag{5}$$

In the static case t is clearly the same as the electron-scattering optical depth, while in the expanding case t is less than the electron optical depth by a possibly large factor.

In order to obtain the total force due to an ensemble of lines, one simply sums equation (1) over all the lines. The factor F_c in equation (1) is the continuum flux per interval of frequency at the frequency of the line. It is

convenient to express this as a multiple of the total flux F, and also to remove a factor σ_e from the summation. Thus we have the following expression for the total force due to lines

$$f_{\rm rad} = \frac{\sigma_e F}{c} M(t) . \tag{6}$$

The first factor, $\sigma_e F/c$, is the force due to continuous absorption. The force multiplier function $M(t)$, which expresses the effect of all the lines, is given by

$$M(t) = \sum_{\rm lines} \frac{F_c \Delta\nu_D}{F} \min\left(\frac{1}{\beta}, \frac{1}{t}\right) . \tag{7}$$

The quantity β is related to the atomic populations and the oscillator strength by

$$\frac{1}{\beta} = \frac{\pi e^2}{mc} gf \frac{N_l/g_l - N_u/g_u}{\rho\sigma_e} \frac{1}{\Delta\nu_{\rm D}} , \tag{8}$$

and $\Delta\nu_{\rm D}$ is the Doppler width

$$\Delta\nu_{\rm D} = \nu_0 v_{\rm th}/c . \tag{9}$$

If the depth variable t is as large as unity, which must occur somewhere near the stellar photosphere, then we see from equation (7) that the force multiplier is no larger than the fraction of the continuum flux which is blocked by lines, each line blocking a band one thermal Doppler width in extent. In fact, this fraction is quite small, of the order of 1 percent, so the force multiplier is small compared with unity and the line force is a minor perturbation to the force due to continuous absorption. In the limit that the optical depth parameter t is very small, the force multiplier becomes

$$M(0) = \sum_{\rm lines} \frac{F_c}{F} \frac{\pi e^2}{mc} gf \frac{N_l/g_l - N_u/g_u}{\rho\sigma_e} . \tag{10}$$

If we take the typical width of the continuous energy distribution to be about $2.5kT_{\rm eff}/h$, which is therefore a typical value of F/F_c, and also invoke the oscillator strength sum rule, we find the following maximum value for the force multiplier

$$M_{\rm max} \approx 0.7 \times 10^8 (10^4 \,^\circ {\rm K}/T_{\rm eff}) X , \tag{11}$$

where X is the fraction of all the atoms in the gas which are able to absorb effectively in the spectral region where most of the flux is emerging. In stars of spectral type O the value of X may be about 10 percent of the abundance of C, N, and O, because for most of the ions of these elements the strong lines have energies (≈ 10 eV) that are about one-fifth of the ionization energy (≈ 50 eV), or about three or four times kT at the temperature for which the ion is most abundant; in other words, the strong lines of these ions tend to coincide with the Planck maximum. This means that X is about 10^{-4}, so that $M_{\rm max}$ is of the order of 10^3.

This value of $M_{\rm max}$ should be compared with the typical ratio of the radiation force for electron scattering alone to the gravity, $\Gamma = 0.05$ to 0.5. It appears that the force exerted in the lines will exceed the gravity by about two orders of magnitude at small optical depths in an O star, even if the atmosphere is assumed to be static. Thus, for O stars, *a static atmosphere is not possible*; there is no mechanism which can prevent the ejection of the surface layers. This contradicts the conclusion of Lucy and Solomon, who assumed that the force was negligible in the absence of a velocity field.

We have used equations (7)–(9) to evaluate the force multiplier for the lines of the C III spectrum. The additional assumptions we have made are:

1) The levels of C^{+2} are populated as in LTE, using Boltzmann's equation with temperature T.

2) The flux distribution in the continuous spectrum, F_c/F, is taken to be the same as for a blackbody at temperature T.

3) The abundance of C^{+2} relative to hydrogen is taken to be 10^{-3}, which is approximately the total abundance of C, N, and O.

Assumptions (1) and (3) are serious; if it were possible to eliminate these assumptions with our present knowledge, we would definitely do so. Unfortunately, we cannot at this time perform the detailed excitation calculations necessary to eliminate (1), for lack of the immense quantity of atomic data that would be required. We cannot treat the other ions, necessary to dispense with assumption (3), since the oscillator strengths are not available, and also since the ionization balance problem is almost as severe as the excitation problem. Assumption (2) is probably a reasonable approximation. In any event, it would be a simple matter to use the flux distribution for a model atmosphere; we have not done so since the inaccuracy introduced by using a Planck function is minor compared with that due to (1) and (3).

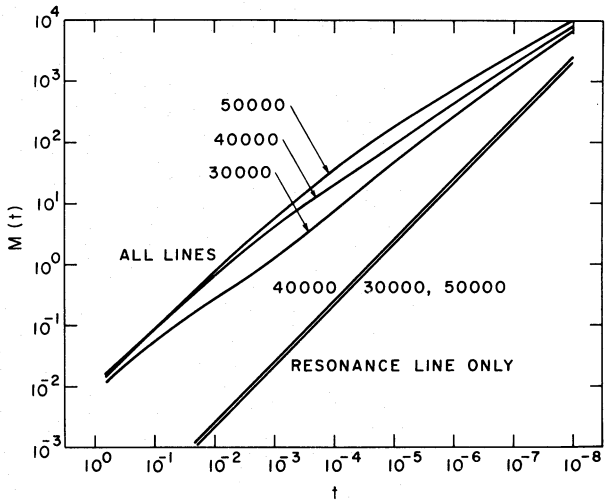

FIG. 1.—Factor giving the increase in radiation force when lines are included, as a function of optical depth. The ordinate is the function M defined in the text (eq. [6]), and the abscissa is the optical depth parameter t, equation (5). The curves labeled "all lines" were computed using 900 multiplets of C III; the curves "resonance line only" included just the C III resonance line λ977. The multiplier was computed for three temperatures T, as indicated in the figure.

The force multiplier we have calculated is shown in figure 1 as a function of the depth parameter t for temperatures $T = 30{,}000°$, $40{,}000°$, and $50{,}000°$ K. The calculated values do indeed span roughly the range estimated above, and, interestingly, vary approximately as a power of the optical depth in the intermediate range, the power being negative but greater than -1. For each of the three values of T we have fitted the multiplier to the formula

$$M(t) = kt^{-\alpha}, \tag{12}$$

where the constants k and α are adjusted to give agreement in the region where $M(t)$ is about 5; this is the region that is most important for the model to be described below. The constants that were determined are given in table 1. For the model calculation, rather than use the constants of table 1 we take the rounded numbers $k = 1/30$ and $\alpha = 0.7$, to give the following formula:

$$M(t) = \tfrac{1}{30}t^{-0.7}. \tag{13}$$

Equation (13) represents M for $T = 40{,}000°$ K to an accuracy of 1 percent in the range $M = 3$ to 5, while it overestimates M at $30{,}000°$ K by about three times, and underestimates M at $50{,}000°$ K by 30 percent.

Figure 1 also shows the multiplier which results if only the C III resonance line λ977 is allowed to contribute. The force at the depth $t = 10^{-3}$ is about 100 times less than when all lines enter. The reason is essentially that there are 100 optically thick lines favorably situated in the flux distribution at this value of t, of which λ977 is but one. The resonance line has an optical depth of a few times 10^6 at $t = 10^{-3}$, so it is possible for strong lines with excitation potentials of the lower level of 40 eV or more to still be optically thick. The factor of 100 by which the subordinate lines magnify the force will be seen below to produce a hundredfold increase in the rate of mass loss over the Lucy and Solomon models.

It is of some interest to see how the force responds to changes in the abundance of the absorbing ion, and to changes in the thermal Doppler width. If X is the ionic abundance, then we see from equations (7)–(9) that

$$M(X', v_{\rm th}', t) = \frac{X'}{X} M\left(X, v_{\rm th}, \frac{X'}{X}\frac{v_{\rm th}}{v_{\rm th}'}t\right), \tag{14}$$

TABLE 1

$M(t) = kt^{-\alpha}$

T (° K)	k	α
30,000.....	0.0076	0.742
40,000.....	0.0026	0.737
50,000.....	0.0021	0.811

so that the constant k in equation (12) varies with X and $v_{\rm th}$ as

$$k \propto X^{1-\alpha} v_{\rm th}{}^{\alpha} . \tag{15}$$

We see that the force due to the lines of any ion then varies as the ionic abundance to quite a small power, 0.25, to 0.3. In the expanding atmosphere we shall be mostly concerned with, t is proportional to $v_{\rm th}$ (cf. eq. [5]) and therefore the force is independent of $v_{\rm th}$ as we should have expected.

As a consequence of the force per ion varying as a low power of the ionic abundance, the force is actually increased by dividing the abundance over several ions. As an example, we consider the ionization state of the stellar material for $T = 35{,}000°$ K and $N_e = 10^{11}$ cm^{-3}, according to LTE. We find C IV and C V in the proportions 0.012:0.988; N III, N IV, N V, and N VI in the ratio 0.000024:0.183:0.816:0.001; and O III, O IV, O V, and O VI in the ratio 0.000276:0.726:0.274:0.000007. The ions of the Li and He isoelectronic sequences have spectra which are poorly distributed for producing force, so we suppose these may be neglected. The ions of the Be, B, and C sequences we suppose to be like C III. For the elemental abundances we assume C:N:O = 0.28:0.085:0.63, and for α we take 0.75. The result is that the force contributions are N III, 0.038; N IV, 0.353; O III, 0.115; O IV, 0.822; O V, 0.645; the unit of force is that which would result if one of the Be-, B-, or C-like ions were given the combined abundance. The total force is 1.97, or twice as great as if all the abundance were lumped into one ion, notwithstanding that half of the abundant ions do not contribute to the force.

III. THEORY OF A LINE-DRIVEN STELLAR WIND

We suppose that the stellar envelope can be described as a steady radial fluid flow with the temperature distribution $T(r)$ specified in advance. The forces that must be taken into account are (1) gravity, (2) gas pressure, (3) continuum radiation pressure, which derives mostly from the Thomson scattering opacity, and (4) the force by radiation in the lines. The continuum opacity sources other than electron scattering, e.g., bound-free absorption are negligible in the part of the envelope where the flow velocity is appreciable. The reason for taking a specified temperature distribution is that the time scale for radiative equilibrium to be established is always small compared with the time for the density of a parcel of gas to fall by a factor e as it flows outward; this condition fails for sufficiently large distances from the star, but not within 10 or more stellar radii of the photosphere. The fluid approximation is an excellent one at the densities (10^{11} cm^{-3}) which characterize the flow, especially since the gas is highly ionized.

The two equations which determine the flow are of mass conservation

$$\frac{d\mathfrak{M}}{dt} = 4\pi r^2 \rho v = \text{constant} , \tag{16}$$

and of momentum balance

$$v \frac{dv}{dr} = -\frac{G\mathfrak{M}}{r^2} + \frac{\sigma_e L}{4\pi r^2 c}[1 + M(t)] - \frac{1}{\rho}\frac{dp_g}{dr} . \tag{17}$$

Here L and $\mathfrak{M}$ are the luminosity and mass of the star. The equation of state is

$$p_g = \rho a^2 ; \tag{18}$$

and a, the isothermal sound speed, is supposed to be given as a function of radius. The force due to gas pressure is found from equations (16) and (18):

$$-\frac{1}{\rho}\frac{dp_g}{dr} = \frac{a^2}{v}\frac{dv}{dr} + \frac{2a^2}{r} - \frac{da^2}{dr} . \tag{19}$$

The multiplier M, which expresses the effect of the lines, is given by the approximate formula (12) in which t is found from the velocity gradient by equation (5) in the expanding atmosphere case. The density, which enters in equation (5), can be eliminated in favor of the velocity, radius, and rate of mass loss with equation (16). This gives the equation for the velocity

$$\left(v - \frac{a^2}{v}\right)\frac{dv}{dr} = -\frac{G\mathfrak{M}(1-\Gamma)}{r^2} + \frac{2a^2}{r} - \frac{da^2}{dr} + \frac{\Gamma G\mathfrak{M}k}{r^2}\left[\frac{4\pi}{\sigma_e v_{\rm th}(d\mathfrak{M}/dt)}\right]^{\alpha}\left(r^2 v \frac{dv}{dr}\right)^{\alpha} , \tag{20}$$

where the parameter Γ is

$$\Gamma = \frac{\sigma_e L}{4\pi G\mathfrak{M}c} . \tag{21}$$

The discussion is very much facilitated by the introduction of a new set of variables, w, u, and h, defined by

$$w = \tfrac{1}{2}v^2 , \tag{22}$$

$$u = -1/r , \tag{23}$$

and

$$h = -G\mathfrak{M}(1 - \Gamma) + 2a^2 r - r^2 \frac{da^2}{dr} . \tag{24}$$

Since a is a known function of r, h is also known as a function of r, and hence of u. The rate of mass loss can be absorbed in a constant C:

$$C = \Gamma G\mathfrak{M}k\left[\frac{4\pi}{\sigma_e v_{\rm th}(d\mathfrak{M}/dt)}\right]^{\alpha} . \tag{25}$$

Let w' stand for dw/du. Then equation (20) can be written

$$F(u, w, w') \equiv (1 - a^2/2w)w' - h(u) - C(w')^{\alpha} = 0 . \tag{26}$$

$F(u, w, w')$, defined by equation (26), is a well-behaved function of its arguments, if w and w' are positive; but in contrast to the solar wind theory F is not a linear function of the derivative w'. If one inserts various values of u and w in equation (26) and attempts to solve it for w', he may find zero, one, or two solutions, depending on which values are chosen, the behavior of the function $h(u)$, and the value of the constant C. It is not hard to show from equation (26) that the cases are (cf. fig. 3)

I. $w < \frac{1}{2}a^2$ and $h < 0$. One solution for w'.

II. $w > \frac{1}{2}a^2$, $h < 0$, and $(1 - a^2/2w) < \alpha(1 - \alpha)^{(1-\alpha)/\alpha}C^{1/\alpha}(-h)^{-(1-\alpha)/\alpha}$. Two solutions for w'.

III. $w > \frac{1}{2}a^2$ and $h > 0$. One solution for w'.

IV. $w > \frac{1}{2}a^2$, $h < 0$, and $(1 - a^2/2w) > \alpha(1 - \alpha)^{(1-\alpha)/\alpha}C^{1/\alpha}(-h)^{-(1-\alpha)/\alpha}$. No solution.

V. $w < \frac{1}{2}a^2$ and $h > 0$. No solution.

In region II, w' is double valued. The two branches of w' as a function of u and w join along the line that separates regions II and IV. One of these branches, the one that gives the smaller w', is continuous with the unique solution in region I, while the branch that gives the larger w' is continuous with the solution in region III. The border between regions II and IV is the locus of singular points of the differential equation. It is defined by equation (26) and the following condition:

$$\frac{\partial F(u, w, w')}{\partial w'} = \left(1 - \frac{a^2}{2w}\right) - \alpha C(w')^{\alpha - 1} = 0 . \tag{27}$$

In order to map the singular locus and delineate the five regions we must investigate the properties of $h(u)$.

Far from the star the temperature varies, if at all, more slowly than $r^{-1/2}$, so the second and third terms on the right side of equation (24) sum to a number between 1.5 and 2 times $a^2 r$. We recall that a^2 is very much less (a few hundred times) than the square of the escape velocity, so h is very nearly $-G\mathfrak{M}(1 - \Gamma)$ from 1 or 2 stellar radii out to several hundred stellar radii. Eventually, however, $a^2 r$ exceeds $G\mathfrak{M}(1 - \Gamma)$ and h becomes positive. Interior to the sonic point (where $v = a$) the run of pressure closely approximates that for hydrostatic equilibrium, so we can express h in terms of the logarithmic temperature gradient, $\nabla \equiv d \log T/d \log p_g \approx 0.25$;

$$h = -G\mathfrak{M}(1 - \Gamma)\left[1 - \nabla - \frac{2a^2 r}{G\mathfrak{M}(1 - \Gamma)}\right] \approx -G\mathfrak{M}(1 - \Gamma)(1 - \nabla) . \tag{28}$$

So we suspect that h must begin, at small radius, at the value $-G\mathfrak{M}(1 - \Gamma)(1 - \nabla)$, decrease to $-G\mathfrak{M}(1 - \Gamma)$ as the photosphere is passed, then increase again and tend to $+\infty$ at large r. In order that region IV exist, h must be more negative than a critical value that depends on C,

$$h < h_c = -\alpha^{\alpha/(1-\alpha)}(1 - \alpha)C^{1/(1-\alpha)} . \tag{29}$$

If the rate of mass loss is too little, C will be too great, and there will be no values of h that meet condition (29). We suppose that C is such that condition (29) is satisfied for u between u_1 and u_2. The function $h(u)$ is sketched in figure 2.

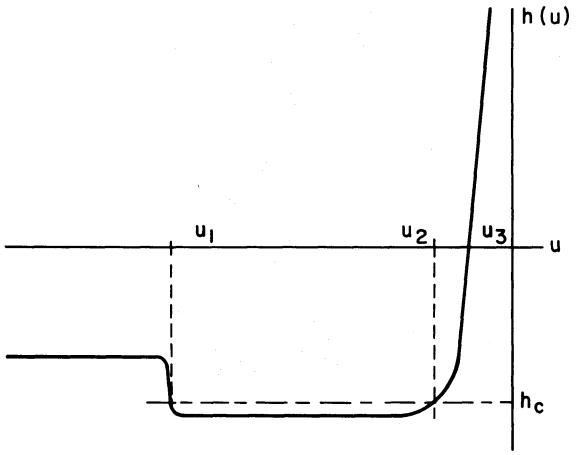

FIG. 2.—Sketch of the force function h versus $u = -1/r$. The quantity h/r^2 is the net force per unit mass due to gravity, continuum radiation pressure, and the parts of the gas pressure gradient due to the temperature gradient and to the curvature term in the velocity divergence. The center of the star lies at infinity toward the left, and infinite radius occurs at the h axis. The quantity h_c is the critical value of h for region IV of the solution of the flow equation to exist; it is given by equation (29). The quantity h assumes the value h_c at u_1 and u_2, and vanishes at u_3.

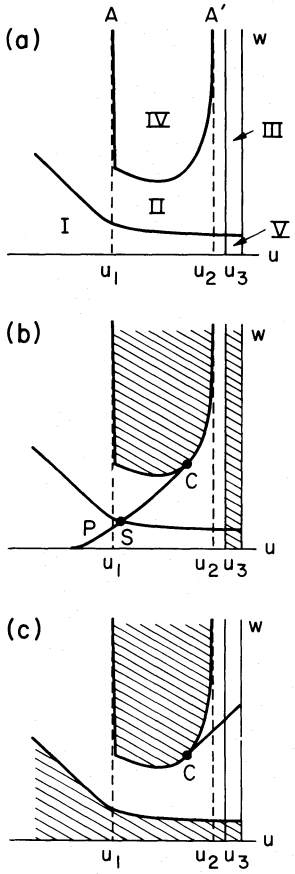

FIG. 3.—(*a*) Sketch of the velocity-radius diagram ($w = v^2/2$, $u = -1/r$) showing five regions for dw/du as a function of w and u. In regions IV and V dw/du does not exist, in regions I and III there is a unique dw/du, and in region II dw/du is double-valued. The curve that separates regions I and V from regions II and III is the sonic line, $v = a$. The curve AA′ that separates regions II and IV is the locus of singular points of the differential equation. Vertical lines mark the values of u_1, u_2, and u_3, defined in fig. 2. (*b*) The part of (w, u)-diagram that is *not* shaded is the region in which the smaller of the two branches of the function $w'(w, u)$ is defined, comprising regions I and II. The part of the regular solution of the flow equation for radii smaller than the singular radius lies on this branch, and is shown as the curve PSC. P indicates the photosphere, which is near $u = u_1$, S is the sonic point, and C is the singular point. (*c*) The part of the diagram that is not shaded is the region in which the larger branch of the w' function is defined, and consists of regions II and III. This branch contains the part of the regular solution of the flow equation for radii greater than that of the singular point, indicated by the diagonal line extending upward from C, the singular point. The curve PSC and its continuation is the unique solution that is subsonic at small radius and extends to arbitrarily large radius.

From the information given in figure 2, it is possible to map the five regions of the (w, u)-diagram. These are shown in figure 3*a*. The unshaded part of figure 3*b* indicates the domain of the small branch of the w' function, and, as described above, it extends into region I. Figure 3*c* likewise shows the domain of the large branch of the function, which extends into region III. An acceptable stellar wind solution must be subsonic at small r, and extend with high velocity to arbitrarily large radius. Therefore, it must begin in region I on the small branch of w', and end in region III on the large branch of w'. Since the two branches join *only* on the locus of singular points, the solution curve must graze the singular locus, and pass from the small branch to the large branch at the point of contact, which is the singular point of the solution. Thus the part of the solution curve interior to the singular point lies on the small branch of w' and the part exterior to the singular point lies on the large branch. This is indicated in figures 3*b* and 3*c*.

Not every point on the singular locus can be the singular point of a solution. In fact, there is a unique point. The reason is that the solution curve must be tangent to the singular locus at the point of contact; if it were not, w' would be discontinuous. To find the criterion for w' to be continuous we suppose that $w(u)$ is a solution of the differential equation for which $w''(u)$ exists everywhere. Then since

$$F[u, w(u), w'(u)] = 0\,, \tag{30}$$

we may differentiate with respect to u and find

$$\frac{\partial F}{\partial u} + w'\frac{\partial F}{\partial w} + w''\frac{\partial F}{\partial w'} = 0\,. \tag{31}$$

At the singular point, defined as the point where $\partial F/\partial w'$ vanishes, we then have

$$\frac{\partial F}{\partial u} + w'\frac{\partial F}{\partial w} = 0\,. \tag{32}$$

Equations (26), (27), and (32) determine the singular point, so that u, w, and w' can be found if C is given; or, as we shall do, w, w', and C can be found if u is given. We might point out that if the rate of mass loss is so small that region IV does not exist, it is then impossible to find a solution of the equation that meets the boundary conditions. The situation sketched in figure 2, is, in fact, the only one that leads to an acceptable solution, with a singular radius comparable with the photospheric radius.

When the explicit form of the function F is put into equation (32) the following equation results:

$$-\frac{w'}{2w}\frac{da^2}{du} - \frac{dh}{du} + \frac{a^2}{2w^2}(w')^2 = 0\,, \tag{33}$$

which is a quadratic equation for w'/w with known coefficients. We expect dh/du to be positive at the singular point (cf. figs. 2 and 3), so the positive solution for w'/w is given by

$$\frac{w'}{w} = \frac{1}{2a^2}\frac{da^2}{du} + \left[\left(\frac{1}{2a^2}\frac{da^2}{du}\right)^2 + \frac{2}{a^2}\frac{dh}{du}\right]^{1/2}. \tag{34}$$

If C is eliminated between equations (26) and (27), we find

$$\frac{w'}{w} = -\frac{\alpha}{1-\alpha}\frac{h}{w - \frac{1}{2}a^2}\,, \tag{35}$$

so w at the singular point is given by

$$w = \tfrac{1}{2}a^2 - \frac{\alpha}{1-\alpha}h\left\{\frac{1}{2a^2}\frac{da^2}{du} + \left[\left(\frac{1}{2a^2}\frac{da^2}{du}\right)^2 + \frac{2}{a^2}\frac{dh}{du}\right]^{1/2}\right\}^{-1}, \tag{36}$$

and w' is

$$w' = \frac{1}{4}\frac{da^2}{du} + \left[\left(\frac{1}{4}\frac{da^2}{du}\right)^2 + \frac{a^2}{2}\frac{dh}{du}\right]^{1/2} - \frac{\alpha}{1-\alpha}h\,. \tag{37}$$

The value of C follows from (27), (35), and (37), and is

$$C = -\frac{1}{1-\alpha}h\left\{\frac{1}{4}\frac{da^2}{du} + \left[\left(\frac{1}{4}\frac{da^2}{du}\right)^2 + \frac{a^2}{2}\frac{dh}{du}\right]^{1/2} - \frac{\alpha}{1-\alpha}h\right\}^{-\alpha}, \tag{38}$$

so that the rate of mass loss, found from equation (25), is

$$\frac{d\mathfrak{M}}{dt} = \frac{4\pi}{\sigma_e v_{\rm th}} (\Gamma G\mathfrak{M}k)^{1/\alpha}(1-\alpha)^{1/\alpha}(-h)^{-1/\alpha}\left\{\frac{1}{4}\frac{da^2}{du} + \left[\left(\frac{1}{4}\frac{da^2}{du}\right)^2 + \frac{a^2}{2}\frac{dh}{du}\right]^{1/2} - \frac{\alpha}{1-\alpha}h\right\}. \tag{39}$$

When the original variables are restored, equations (36), (37), and (39) become

$$v^2 = a^2 + \frac{\alpha}{1-\alpha}[2G\mathfrak{M}(1-\Gamma)/r - 4a^2 + 2rda^2/dr]\left\{\frac{r}{2a^2}\frac{da^2}{dr} + \left[\left(\frac{r}{2a^2}\frac{da^2}{dr}\right)^2 + 4 - \frac{2r^2}{a^2}\frac{d^2a^2}{dr^2}\right]^{1/2}\right\}^{-1}, \tag{40}$$

$$r^2 v\frac{dv}{dr} = \frac{r^2}{4}\frac{da^2}{dr} + \left[\left(\frac{r^2}{4}\frac{da^2}{dr}\right)^2 + a^4r^2 - \frac{a^2r^4}{2}\frac{d^2a^2}{dr^2}\right]^{1/2} + \frac{\alpha}{1-\alpha}\left[G\mathfrak{M}(1-\Gamma) - 2a^2r + r^2\frac{da^2}{dr}\right], \tag{41}$$

and

$$\frac{d\mathfrak{M}}{dt} = \frac{4\pi}{\sigma_e v_{\rm th}} (\Gamma G\mathfrak{M}k)^{1/\alpha}(1-\alpha)^{1/\alpha}\left[G\mathfrak{M}(1-\Gamma) - 2a^2r + r^2\frac{da^2}{dr}\right]^{-1/\alpha}$$
$$\times\left\{\frac{r^2}{4}\frac{da^2}{dr} + \left[\left(\frac{r^2}{4}\frac{da^2}{dr}\right)^2 + a^4r^2 - \frac{a^2r^4}{2}\frac{d^2a^2}{dr^2}\right]^{1/2} + \frac{\alpha}{1-\alpha}\left[G\mathfrak{M}(1-\Gamma) - 2a^2r + r^2\frac{da^2}{dr}\right]\right\}. \tag{42}$$

The radius that appears in these equations is the singular radius, which will be denoted by r_c, to distinguish it from the sonic point radius r_s (see fig. 3*b*). As we will show, the singular radius is 1.5 to 2 times the photospheric radius, so it is certainly true that $a^2 \ll G\mathfrak{M}(1-\Gamma)/r_c$. This allows a considerable simplification of equations (40)–(42). We suppose that near the singular point the temperature follows a power law in radius, so

$$a^2 \propto T \propto r^{-n}. \tag{43}$$

Then we find

$$v^2 = \frac{\alpha}{1-\alpha}\frac{2G\mathfrak{M}(1-\Gamma)/r_c}{-\frac{1}{2}n + [\frac{1}{4}n^2 + 4 - 2n(n+1)]^{1/2}}, \tag{44}$$

$$r^2 v\frac{dv}{dr} = \frac{\alpha}{1-\alpha}G\mathfrak{M}(1-\Gamma), \tag{45}$$

and

$$\frac{d\mathfrak{M}}{dt} = \frac{4\pi G\mathfrak{M}}{\sigma_e v_{\rm th}}\alpha(1-\alpha)^{(1-\alpha)/\alpha}k^{1/\alpha}\Gamma^{1/\alpha}(1-\Gamma)^{-(1-\alpha)/\alpha}. \tag{46}$$

Furthermore, if v is large compared with a, equation (20) indicates that r^2vdv/dr remains constant until r is as large as $G\mathfrak{M}(1-\Gamma)/a^2$. Therefore, equation (45) is true not only at the singular point, but from somewhere near the sonic point out to many stellar radii. Equation (45) can then be integrated with equation (44) to fix the constant of integration. This gives the velocity law

$$v^2 = \frac{\alpha}{1-\alpha}2G\mathfrak{M}(1-\Gamma)\left(\frac{1}{r_s} - \frac{1}{r}\right), \tag{47}$$

where we have identified the radius where the velocity vanishes in this approximation with the sonic radius, and the ratio of singular radius to sonic radius

$$\frac{r_c}{r_s} = 1 + \frac{1}{-\frac{1}{2}n + [\frac{1}{4}n^2 + 4 - 2n(n+1)]^{1/2}}. \tag{48}$$

The value of n is likely to fall between 0 and 0.5, so the singular radius will lie between 1.5 and 1.74 times the sonic radius. The sonic radius is essentially the same as the photospheric radius since the density rises very rapidly interior to the sonic point.

The stellar model is parametrized with the values of L, $\mathfrak{M}$, and the photospheric radius. To a first approximation one can identify the photospheric radius with the sonic radius and use equation (48) to estimate r_c. Equations (40)–(42) then define all the variables at the singular point. Then one can integrate equation (20) numerically in each direction from the singular point, taking care to select the correct branch of dv/dr for each integration, i.e., the small branch for the inward integration and the large branch for the outward integration. This yields a complete model. The exact relation found between optical depth and radius from the integrations can then be examined to see if the photospheric radius has the value desired; if not, r_c can be adjusted and the process repeated. When this

process has converged, the density structure can be used in a model atmosphere code to find an improved temperature relation satisfying radiative equilibrium, and so on. Because the rate of mass loss and the velocity structure are quite insensitive to the temperature law, iteration of the temperature distribution converges very rapidly.

IV. A MODEL ENVELOPE FOR AN O5f STAR

We have used the theory of the preceding section to construct a stellar wind model for a star with the parameters $\mathfrak{M} = 60\,\mathfrak{M}_\odot$, $L = 9.66 \times 10^5\,L_\odot$, $\Gamma = 0.4$, $T_{\rm eff} = 49{,}290°$ K, $\log g = 3.94$, $R = 9.585 \times 10^{11}$ cm $= 13.8\,R_\odot$. These correspond approximately to a main-sequence star of spectral class O5, although the mass chosen may be too small if evolutionary tracks are to be believed, and $100\,\mathfrak{M}_\odot$ might be more nearly correct. In view of the uncertainties in the radiation force calculation, we have taken equation (13) for the force multiplier. The temperature distribution was iterated once using the spherical LTE atmosphere code of Castor (1974*b*). This code was modified so that radiative equilibrium was imposed as usual, but hydrostatic equilibrium was obeyed only interior to the photosphere; exterior to the photosphere the density was taken from a previous stellar wind model which had assumed a constant temperature equal to 50,000° K. The LTE assumption gives temperatures which are certainly too small in the outer envelope, of the order 27,000°–38,000° K, but the temperature in this region has little effect on the solution. Between the sonic point and the photosphere the temperature varies from 38,000° to 50,000° K, and the LTE assumption should be adequate in this region. Although equation (20) is used even in regions where the high-velocity approximation (eq. [3]) is inapplicable, this introduces no error, since the line force becomes small where the approximation is still valid.

We find for the rate of mass loss the value

$$\frac{d\mathfrak{M}}{dt} = 4.16 \times 10^{20}\ \mathrm{g\ s^{-1}} = 6.61 \times 10^{-6}\,\mathfrak{M}_\odot\ \mathrm{yr^{-1}} = \frac{\mathfrak{M}}{9.08 \times 10^6\ \mathrm{years}}\,.$$

This value of the rate of mass loss is also 0.5 of the value $L/v_\infty c$. This indicates that roughly half of the original momentum carried by the radiation has been given to the matter, and that half of the total continuum flux has been blocked by lines. Thus the driving mechanism is operating near maximum efficiency. Stothers (1966) gives main-sequence lifetimes for $60\,\mathfrak{M}_\odot$ and $100\,\mathfrak{M}_\odot$ stars of about 3×10^6 yr and 2.5×10^6 yr, respectively. (Notice that from eq. [46] the rate of mass loss is proportional to the stellar mass.) Therefore we find that the star should lose from one-fourth to one-third of its mass during its main sequence phase of evolution,

$$\frac{t_{\rm MS}}{\mathfrak{M}}\frac{d\mathfrak{M}}{dt} \approx \tfrac{1}{4} \rightarrow \tfrac{1}{3}\,.$$

This result, if it is correct, will have a major effect on the evolution of the star. Stothers's models indicate that nuclear burning has affected the inner 63 percent of the stellar mass substantially, and the inner 81 percent of the mass to some extent, by the time the star leaves the main sequence. This opens the possibility that mass loss in an Of star will expose nuclear-processed material at the surface. We will discuss below evidence that suggests the large rate of mass loss given above is correct.

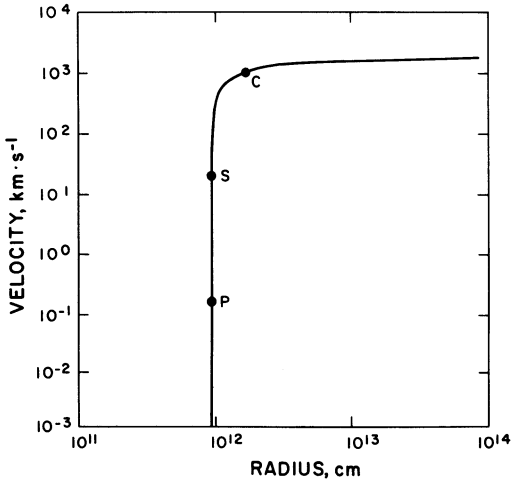

FIG. 4.—Velocity versus radius for the flow model with parameters given in the text. The photospheric radius is made to be a specified value. The temperature distribution is approximately self-consistent with the assumptions of LTE and radiative equilibrium. The point P is the photosphere, S is the sonic point, and C is the singular point, as in fig. 3.

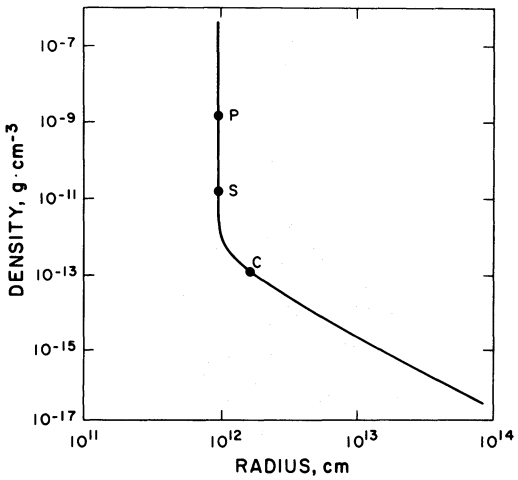

FIG. 5.—Mass density versus radius. Symbols and model the same as in fig. 4.

The structure of the stellar wind is summarized in figures 4–8. The run of velocity with radius, illustrated in figure 4, follows equation (47) fairly well; the terminal velocity is

$$v_\infty = 1515 \text{ km s}^{-1} .$$

Figure 5, which shows the run of density, serves mainly to emphasize that the star has a very decided core-halo structure. The model is clearly separated into a core, which is for all practical purposes the same as a hydrostatic equilibrium model, and an extended envelope in which, after an initial drop, the density falls as r^{-2}. The figure indicates the locations of the photosphere, the sonic point, and the singular point. The mass densities at these three positions are 2.4×10^{-9}, 1.7×10^{-11}, and 1.2×10^{-13} g cm^{-3}, in the same order, or, in terms of electron density, 10^{15}, 10^{13}, and 10^{11} cm^{-3}. The density at the singular point, 10^{11} cm^{-3}, is the characteristic density of the extended envelope.

The optical depth in electron scattering, essentially the same as the total optical depth in the continuum, is 0.049 at the singular point, and 0.157 at the sonic point. This is large enough to affect the radiation field in the continuum; this point is investigated in the next section. In figure 6 the velocity is shown as a function of the optical depth in electron scattering. Interestingly, it is very nearly a linear function. This is in fact a simple consequence of equation (45). From equation (3) we then see that the line optical depth varies in the stellar envelope only as the relative abundance of absorbing ions varies. If the abundance is constant, as for the resonance line of a prevalent ion, then the line is formed equally from all parts of the envelope, so the profile width will be of the order of the terminal velocity. If the abundance of absorbers declines with radius, the low-velocity region will be emphasized more than the high-velocity region. The hydrogen and helium lines fall into the latter category.

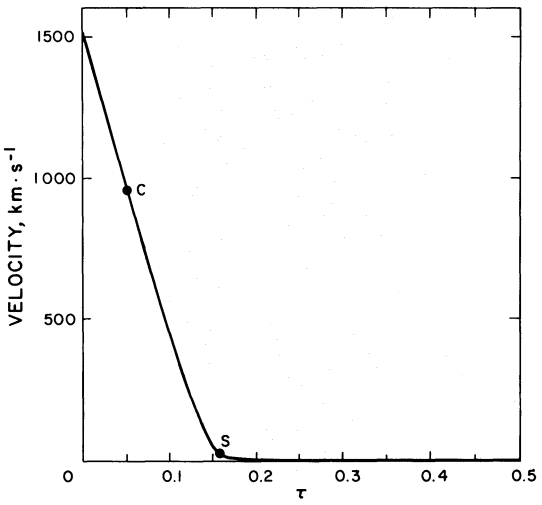

FIG. 6.—Velocity versus optical depth in electron scattering (continuum optical depth). Symbols and model as in fig. 4.

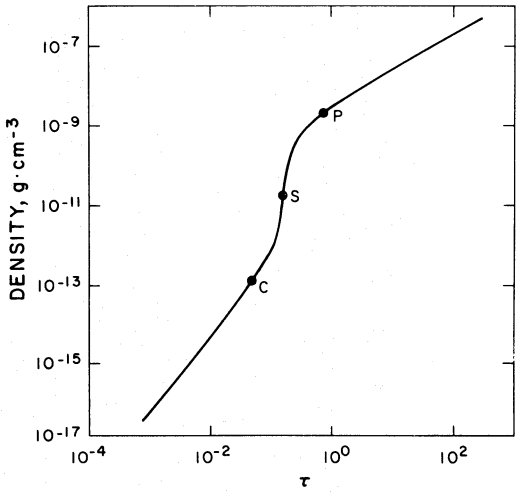

FIG. 7.—Mass density versus electron scattering optical depth. Symbols and model as in fig. 4.

The plot of density versus optical depth, figure 7, shows a sharp break between core and envelope. The middle of the transition region is marked by the sonic point. It is apparent that there is very little material with an intermediate density, moving at a moderate velocity. The spectrum can be expected to be dominated by features formed either inside or outside the transition region.

Figure 8 shows the force multiplier M as a function of optical depth. The bifurcation of the star into core and envelope is striking. In the core, the line force is negligible; at the photosphere, for example, the multiplier is about 0.002. In the envelope the multiplier is large and almost constant, typically about five, which makes the line force alone twice the gravity; when the line force is augmented by the continuum radiation force, the result is an outward acceleration of the material equal to 1.4 times the acceleration of gravity. Only in the transition region is the line force significant, but such that the total radiation force is less than the gravity. For this reason the assumption by Mihalas and Hummer (1974*a*, *b*) that the line force could be represented by a slowly decaying function of optical depth, maximizing at a value compatible with hydrostatic equilibrium, does not seem appropriate. Their treatment does not produce core-halo models, but rather models with a fairly uniform extension. Thus they overestimate the effect on the continuum, and underestimate the effect on the strong lines. The noticeable reddening of the continuum they find, and the inability to produce Balmer lines in emission may be symptoms of this defect.

The near constancy of $M(t)$ at the value 5 is the justification for fitting k and α (in principle) near that value.

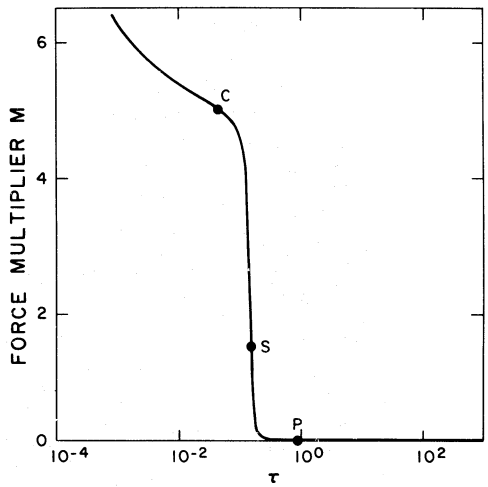

FIG. 8.—Force multiplier M versus electron scattering optical depth. Symbols and model as in fig. 4. $M + 1$ is the total radiation force in units of the force due to electron scattering alone. $1 - 0.4(M + 1)$ is, for this model, the effective gravity in units of $G\mathfrak{M}/r^2$ and vanishes very near the sonic point.

V. SPECTRAL MODIFICATIONS PRODUCED BY THE STELLAR WIND

As a by-product of the stellar wind calculation we have computed a model atmosphere consistent with the stellar wind density distribution, on the assumptions of LTE and radiative equilibrium but accounting for spherical symmetry. The continuous spectrum can be described with the variation of spectral luminosity, effective radius, and brightness temperature as a function of wavelength. (The latter two quantities are defined by Castor 1974*b*.) Table 2 gives a comparison of these quantities for the stellar wind model, and a hydrostatic equilibrium model with very similar parameters ($T_{\rm eff}$ = 49,931° K instead of 49,290° K). (The line force must be neglected to obtain a hydrostatic model.) It is apparent that the spectral distribution of the emergent luminosity is the same for the two models, to observational accuracy, except in the unobservable far-ultraviolet. For both models the spectral gradient between the visual and blue wavelengths indicates a temperature of about 50,000° K (48,000° K for the hydrostatic model, and 51,000° K for the flow model).

The principal difference that *does* exist between the hydrostatic and flow models is that the flow model appears *larger*, owing to the scattering envelope. The difference amounts to 13 percent in the visual, when allowance is made for the different photospheric radii. Another model which had a larger optical depth in the envelope (0.27 at the sonic point, instead of 0.16) had an effective radius in the visual 29 percent larger than that of the static model. That particular flow model gave a brightness temperature in the visual of 29,000° K, very similar to the brightness temperature found for ζ Pup, O4f, by Davis *et al.* (1970). The spectral distribution for that model was still the same as for the static model.

The reason why the envelope has so little effect on the continuous spectrum probably lies in the fact that the envelope is so tenuous that very few continuum photons can be created there; the envelope simply acts as a conservative scattering layer added to the outside of the model atmosphere. This simply shifts the optical depth scale by approximately the depth of the layer, so that the same relation between temperature and optical depth obtains as before. We can also see why the effect of the extended scattering region is small if we recall that the reason an extensive absorbing envelope makes the spectrum redder is that it absorbs radiation incident from the photosphere and re-emits it at longer wavelengths owing to the fact that the envelope is necessarily considerably cooler than the photosphere. In the absence of the envelope this effect is much less since the surface temperature is more nearly comparable with that of the photosphere, and if the envelope scatters rather than absorbs it does not occur since the radiation is emitted at the same frequency at which it is absorbed.

This result appears to be in conflict with the conclusion of Mihalas and Hummer (1974*a*), who suggest that the visible spectrum of ζ Pup is affected by intrinsic reddening such as might be produced in a spherical static extended atmosphere, essentially by the mechanism mentioned above. If this mechanism does *not* operate in the expanding envelope model, which we would suppose to be applicable to ζ Pup, then how can we explain the intrinsic reddening? In fact, this reddening may not exist in the *visible* spectrum of ζ Pup. (There is unquestionably a deficiency of ultraviolet flux in ζ Pup.) As figure 1 of Mihalas and Hummer indicates, ζ Pup has a $b - y$ color which is quite blue indeed, but is deficient in $u - b$. However, the four-color observations are affected by contaminating lines, and it may be preferable to examine the spectrophotometric data of Aller, Faulkner, and Norton (1966). We have

TABLE 2

COMPARISON OF THE SPECTRA OF FLOW AND STATIC MODELS

	Hydrostatic Equilibrium			Flow		
λ (Å)	L_ν (ergs s^{-1} Hz^{-1})	$R_{\rm UD}(\nu)$ (10^{11} cm)	$T_b(\nu)$ (° K)	L_ν (ergs s^{-1} Hz^{-1})	$R_{\rm UD}(\nu)$ (10^{12} cm)	$T_b(\nu)$ (° K)
8204.....	4.53×10^{22}	9.248	40,772	4.60×10^{22}	1.069	32,601
5050.....	1.06×10^{23}	9.170	42,154	1.08×10^{23}	1.060	34,651
3647$^+$.....	1.79	9.106	43,121	1.85	1.053	36,316
3647$^-$.....	1.78	9.164	42,538	1.81	1.059	35,657
3037.....	2.35	9.125	43,280	2.40	1.055	36,790
2602.....	2.92	9.089	43,929	3.00	1.052	37,812
1350.....	5.88	8.943	46,940	6.15	1.038	42,511
912.....	7.06	8.882	49,541	7.36	1.032	45,850
911.....	4.62	9.043	43,458	4.65	1.051	40,197
649.....	4.15	8.834	47,225	4.10	1.028	44,214
504.....	3.37	8.714	50,711	3.31	1.015	47,906
344.....	1.85	8.680	56,766	1.79	1.010	54,250
262.....	9.30×10^{22}	8.731	61,918	8.91×10^{22}	1.015	59,563
244.....	7.48	8.747	63,398	7.15	1.017	61,079
228.....	6.02	8.761	64,823	5.74	1.018	62,536
188.....	2.94	8.796	69,283	2.78	1.022	67,074
160.....	1.45	8.817	73,417	1.36	1.025	71,258
102.....	1.09	8.846	87,104	9.87×10^{21}	1.028	84,977
75.....	1.02	8.853	98,562	7.49	1.029	95,553

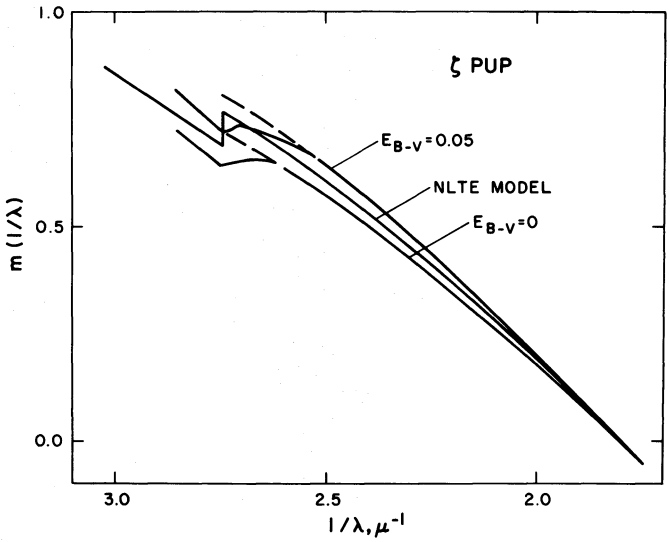

FIG. 9.—Energy distribution in the visible for ζ Pup, O4ef. The data are those of Aller *et al.* (1966), transformed to Hayes's system using ξ^2 Cet. They are plotted for two possible values of the reddening, 0 and 0.05. The model is for 50,000° K and log g = 4.0, from Mihalas (1972). The dashed extensions of the observational curves are for the purpose of computing the Balmer jump.

transformed these data to Hayes's (1970) system using the intermediate star ξ^2 Cet, one of Oke's secondary standards, as suggested by Aller *et al.* The reddening of ζ Pup is certainly very small. We have considered the possibilities that it is unreddened, and that it is reddened by 0.05 mag in $B - V$. For the reddening law we have used Johnson's (1965) determination for the Perseus region, which is typical of normal regions in the Galaxy. The intrinsic energy distributions for the two possible values of the reddening are shown in figure 9, along with the energy distribution for the NLTE/L model with $T_{\rm eff}$ = 50,000° K and log g = 4.0, taken from Mihalas (1972). The agreement is seen to be excellent. The Balmer jump of the model is 0.078 mag, while the observed jump is 0.08 mag. The slope of the Paschen continuum of the model lies midway between the observations for no reddening, and for a $B - V$ excess of 0.05. Brandt *et al.* (1971) have examined the reddening for several B stars in the direction of the Gum nebula. The mean $b - y$ excess of nine stars is 0.03 with a standard deviation of an individual excess of 0.03. The equivalent mean excess in $B - V$ is about 0.04. The conclusion seems to be that the ground-based photometry of ζ Pup is in excellent agreement with the static plane-parallel non–LTE model. To our knowledge ζ Pup has not been observed spectrophotometrically in the red, although Hayes's (1970) and Oke and Schild's (1970) calibrations extend past 1 μ; it would be quite interesting to see if the agreement with the static model persists in this spectral region.

There is no doubt at all that ζ Pup has less flux in the wavelength region around 1500 Å than is expected for the 50,000° K temperature. Heap (1972) has compared the absolute flux of ζ Pup per unit surface area as a function of wavelength, computed using the angular diameter measured by Davis *et al.* (1970), with model atmospheres, and finds a large discrepancy in the case of a 50,000° K, plane-parallel static model. This is also shown by Mihalas and Hummer (1974*b*), who indicate that the discrepancy is eliminated with an extended static model, a conclusion also reached by Castor (1974*b*). We feel that the angular diameter is affected more by the presence of the envelope than is the spectral distribution itself, and so the comparison should properly be made using the relative energy distributions. When this is done, the discrepancy vanishes between 2000 and 3000 Å, is a maximum 35 percent in the range 1400–1700 Å, and 50 percent near 1200 Å. This is still more than can be accounted for with normal line blanketing, such as in the models of Hickok and Morton (1968). We suggest that the line blanketing effect is very much greater in stars with expanding atmospheres, owing to the fact that the velocity of expansion de-saturates the strong lines in much the same way as a microturbulent velocity of the same order of magnitude, and has a similar effect on the curve of growth. Therefore, the large number of lines that are on the flat part of the curve of growth, which were correctly neglected by Morton and his co-workers in static models, now have very large equivalent widths, and consequently dominate the line blanketing problem. Work is now in progress to show that the blocking due to the moderate strength lines of C, N, and O has the correct wavelength dependence to explain the energy distribution of ζ Pup. We already have had an indication that the total amount of blocking is approximately correct. We saw earlier that the momentum carried away from the star by the wind was about half the total momentum in the continuous radiation, indicating that 0.5 of the energy in the continuum is blocked by line absorption. Thus the predicted rate of mass loss is consistent with a flux deficiency of about the magnitude observed.

It is also possible to make rough estimates of the effect the expanding envelope will have on the line spectrum. We have applied the computer code used by Castor and Van Blerkom (1970) in an analysis of two WN-type Wolf-Rayet stars to estimate the populations of the bound states of H and of He^+ at a typical point in the stellar wind

(near a radius equal to two stellar radii). Surprisingly, we find that almost all lines of these two species are optically thin, in the sense that the optical depth defined by equation (3), taking into account the velocity gradient, is small. The result is that the atomic level populations are similar to those in Menzel's case A. (In He^+, the resonance lines are optically thick, so the populations tend toward case B.) As a consequence, we find that the populations are rather insensitive to the temperature of the gas, and are only moderately sensitive to the continuous radiation field, but are quite sensitive to the density, varying as the square. To the extent that the gas temperature does influence the level populations and hence the emission-line strengths, an increase of temperature produces a decrease of bound-state populations and reduces the emission. Therefore, the presence of Balmer line emission in the spectra of Of stars may be cited as evidence that these stars do not possess very hot coronae.

We estimate the emission in Hα from the whole envelope by assuming that the bound-state populations scale as $1/r^4$ (i.e., as the square of the density) and that the line is optically thin. When the total emission in Hα is compared with the continuous flux at the line frequency given by the NLTE/L model, we find an equivalent width of 8.6 Å, in emission. This compares very favorably with the typical emission equivalent widths measured by Conti (1974) in a number of Of stars. We also find in this calculation that the ground state of hydrogen is considerably overpopulated at the typical point in the envelope, with the result that the Lyman lines are in absorption. A similar calculation for the He II spectrum indicates that λ4686 has an equivalent width of 1.7 Å, also in emission. This also is in the range observed for Of stars (cf. Conti and Leep 1974), although larger values are seen in some stars.

The reason Hα is in emission is essentially geometry—that is, the large emitting volume overcomes the feebleness of the emission. The λ4686 line, in contrast, is an intrinsic emission line, although only by a small margin; the excitation temperature for this transition is 43,400° K, while the brightness temperature in the continuum at the frequency of the line is 40,300° K. The case of the $n = 5$ to $n = 4$ transition, λ10,124, is even clearer. For this transition the excitation temperature is 70,500° K, while the brightness temperature in the background continuum is only 38,300° K, so the line must be in emission, at least to the extent that it is formed in the stellar envelope. We estimate its equivalent width to be 5.6 Å. This is to be compared with the value observed for ζ Pup by Mihalas and Lockwood (1972), 1.7 Å. From these results we feel that the stellar wind model is in qualitative agreement with the observations as regards the line spectrum, although quantitatively there may be discrepancies of a factor of 2 or 3. A more definite statement about the comparison of the line spectrum predicted by the model with observation awaits completion of a proper statistical-equilibrium analysis of hydrogen and helium accounting for the accurate radial structure; this work is in progress.

At this point we would like to consider the consequences of a much lower rate of mass loss than the value given earlier. The scattering optical depth in the extended envelope is proportional to the rate of mass loss. The fraction by which the interferometric radius measured in the visible exceeds the photospheric radius is proportional to the scattering optical depth, and therefore is also proportional to the rate of mass loss. If this rate were less than, say, $3 \times 10^{-6}\,\mathfrak{M}_\odot\ \mathrm{yr}^{-1}$, the scattering optical depth would be negligible, and the paradox about the effective temperature of ζ Pup would return. The strengths of the Balmer emission lines are even better indicators than the interferometric radius of the rate of mass loss. A factor-of-2 reduction in the mass loss from the value given earlier would reduce the hydrogen emission by four times, and remove our equivalent-width predictions from the range in which the observations lie. Morton's (1967) analysis of the N V and Si IV resonance lines in the Orion belt stars (O9.5 to B0, Ia to II) also indicated rates of mass loss somewhat larger than $10^{-6}\,\mathfrak{M}_\odot\ \mathrm{yr}^{-1}$. We feel that the rate of mass loss *must* be of the order that we have suggested in order to explain the nature of the Of spectrum.

VI. CONCLUSIONS

The following points summarize the conclusions we have reached in this work:

1. The force on the stellar material produced by radiation in a large number of subordinate lines can be very large, and in an expanding atmosphere is a function of the local velocity gradient. This force makes rather rapid mass loss inevitable in O stars.
2. A new stellar wind theory has been developed which is based on an analytic approximation to this force law. Just as in the usual theory there is a unique solution that passes through a regular singular point, with a definite value of the rate of mass loss, for specified values of the stellar mass, luminosity, and photospheric radius.
3. The terminal velocity in the wind is always somewhat larger than the escape velocity from the photosphere, about 1500 km s^{-1}.
4. The rate of mass loss is large, about $6 \times 10^{-6}\,\mathfrak{M}_\odot\ \mathrm{yr}^{-1}$ for a main-sequence O5 star. The star would lose from one-fourth to one-third of its mass during main-sequence hydrogen burning. There is then the possibility that in some stars nuclear-processed material may be exposed at the surface.
5. The increase in apparent size of the star produced by electron scattering in the envelope can explain the brightness temperature discrepancy found by Davis *et al.* (1970).
6. The continuous energy distribution (in ergs s^{-1} Hz^{-1}) is affected very little by the stellar wind, which is confirmed by the observations of ζ Pup, for which the ground-based spectrophotometry is in excellent agreement with a static, plane-parallel non–LTE model.

7. The emission spectra of H and He^+ formed in the envelope are quite analogous to those in planetary nebulae, and are insensitive to temperature but sensitive to density. The Lyman lines are expected to be in absorption, as observed, although in all stars except ζ Pup possible emission might be hidden by interstellar absorption. The emission strengths of Hα, and of He II $\lambda\lambda$4686, 10,124, are in the range observed for Of stars.

It is encouraging that we obtain agreement of this order in a theory with no adjustable parameters other than the observable mass, luminosity, and effective temperature. In fairness, though, the parameter k in the force law is not well determined, and it would be fortuitous that the value we estimate produces reasonable agreement.

At this point it may be useful to defend a few of the simplifications we introduced earlier, and comment on how some of the approximations may be improved upon in the future.

In equations (1) and (3) we relate the line force to the radial gradient of the velocity. This is correct if the radiation flow is radial, but is an approximation in general. The correct expression for spherical symmetry can be derived from equation (4.12) in Paper I. It expresses the force for an individual line as an angle integral weighted by the intensity of the core radiation, which we assume to be uniform within the cone subtended by the core, and equal to the Planck function. The integrand is the contribution to the force of the radiation which makes a particular angle with the radial direction. This is essentially the same as equations (1) and (3) with the radial-velocity derivative replaced by the directional derivative of the component of velocity in that direction. We can then perform the superposition of all the lines first, and do the angle integration afterward. We find the following formula for the force multiplier corrected for the effect of the finite cone angle:

$$M_{\rm corr}(t) = \frac{2}{1-\mu_c^2}\int_{\mu_c}^{1} \mu d\mu M\left[\frac{(1+\sigma)t}{1+\sigma\mu^2}\right], \tag{49}$$

where

$$\sigma = \frac{d\ln v}{d\ln r} - 1, \qquad \mu_c = (1 - r_P^2/r^2)^{1/2},$$

and r_P is the core radius, identified with the photospheric radius. The function M is the multiplier in the approximation considered earlier. We substitute equation (12) for $M(t)$ and find the relation between the corrected and uncorrected multipliers:

$$\frac{M_{\rm corr}(t)}{M(t)} = \frac{(1+\sigma)^{1+\alpha} - (1+\sigma\mu_c^2)^{1+\alpha}}{(1+\alpha)(1-\mu_c^2)\sigma(1+\sigma)^{\alpha}}. \tag{50}$$

This factor by which the earlier approximation is in error has been evaluated for the model described in § IV. The approximation is worst at the base of the envelope, the sonic point, where the more accurate formula is 40 percent less. The error rapidly decreases, becoming 19 percent where the velocity has risen to 500 km s^{-1}, vanishes where the velocity is 850 km s^{-1}, and never exceeds about 10 percent at any larger radii. Thus the approximation of radially streaming radiation for the line force does not appear to be a major source of error. Similarly, equation (1) itself is a minor source of error. The numerical coefficient in this equation is correct for the rapidly expanding atmosphere, while it is a rough estimate for a static atmosphere. Besides the angle averaging just mentioned, the expression min $(1, 1/\tau_L)$ should be replaced by $[1 - \exp(-\tau_L)]/\tau_L$. The error from this source can be estimated using a simple statistical model of the distribution of lines in strength and frequency. We suppose that the strength and frequency are statistically independent, that the logarithm of the frequency is uniformly distributed, and that the line strength parameter β is distributed according to a power law, so the number of lines in intervals $d\nu$ and $d\beta$ is

$$dN = N_0\beta^{-\alpha}d\beta\frac{d\nu}{\nu}. \tag{51}$$

When equation (51) is combined with equation (7), equation (12) is reproduced, and k is given by

$$k = \frac{v_{\rm th}}{c}\frac{N_0}{\alpha(1-\alpha)}. \tag{52}$$

With the more accurate formula involving the exponential, there is also a factor $\Gamma(1+\alpha)$ in k, which reduces k by 9 percent. This model of the line distribution also explains why k is more sensitive to changes in excitation and abundance than is α: k is fixed by the constant N_0 which depends on those quantities, while α is simply the exponent in the strength law and is independent of the physical conditions.

The uncertainties involving the excitation state of the ions providing the force are especially vexing. We have assumed LTE excitation of the states of C III, and have identified the excitation temperature with the effective temperature of the star. This seems at first sight to produce a considerable overestimate of the actual excitation in the stellar envelope. In fact, we think it is not that bad. First of all, the actual electron temperature in the envelope is high, almost as high as the effective temperature. The reason is the temperature rise toward small

optical depths which occurs because of departures from LTE. This is the mechanism suggested by Cayrel (1963) for part of the temperature rise in the solar chromosphere, and explored by Auer and Mihalas (1969) in the O and B stars. The statistical equilibrium calculation for hydrogen at a representative point in the envelope, mentioned earlier, indicates strong heating in the Lyman continuum even at temperatures above the effective temperature. A more elaborate calculation, to be described in a future communication, indicates a radiative equilibrium temperature between 40,000° and 50,000° K throughout the envelope, for the model described in § IV. Therefore, we may suppose that both the electron temperature and the color temperature of the continuum radiation (with an exception to be mentioned shortly) are approximately equal to the effective temperature.

The thing which prevents the excitation and ionization state of the material from obeying LTE is, of course, that the continuum radiation is dilute. The typical dilution factor W is 0.1. (When the lines are optically thin, such as for hydrogen, the LTE departures are enhanced by the escape of line radiation; for the ions of C, N, and O the lines are optically thick for the most part, and this effect is smaller.) We may estimate the effect of dilution on the state of the gas by assuming that the level populations are determined by photoionization and radiative recombination alone, and we take the photoionization continua to be optically thin. Then we find that the populations nearly obey the Saha-Boltzmann equation at the effective temperature, except that N_e is replaced by N_e/W. Therefore, the excitation state of the material does correspond to LTE at the effective temperature, while the degree of ionization is somewhat less. A complication arises because the temperature of the background continuum drops from 63,000° K to 35,000° K at the He II Lyman edge. Thus it may turn out that the ground state of an ion is overpopulated with respect to the excited states, since it can be ionized only by radiation above the He II edge. This in fact, was the reason for choosing 35,000° K for the sample calculation of the ionization state given in § II. In the likely event that the ground-state photoionization continuum is optically thick and hence in detailed balance, this 35,000° K radiation becomes irrelevant and the ground-state population drops into line with that of the excited states. We note that Morton (1967) found $T_c \approx 26{,}000°$ K from the N V/Si IV ratio in the Orion stars, $T_{\rm eff} \approx 30{,}000°$ K.

We see the main error of our treatment of the excitation not as that a high excitation temperature was used, for that may be justified, but that the high excitation temperature is incompatible with the existence of the chosen ion, C III. If we had studied O IV, an ion expected to be abundant in the envelope, we would have found somewhat fewer well-populated states owing to the fact that excitation potentials are higher in O IV than in C III. It is very hard to estimate the magnitude of this error, but it may easily be a factor of 2 or 3 in k, and will probably eliminate the increase in k by a factor 2 which theinclusion of many ions would produce. At the present we may only say that k is uncertain by a factor of at least 2, and is more likely to lie lower than the value we have used than higher.

For the future we plan first to investigate the statistical equilibrium of hydrogen and helium as a function of radius in the expanding envelope and thereby make definite predictions of the emission-line profiles and strengths. The results of that analysis should provide either strong confirmation or repudiation of the theory of the Of stars proposed in this paper. The study of hydrogen is partly completed, with promising results; they will be described in a subsequent paper. Two further avenues of investigation we are pursuing are (1) a study of the possible instability of the flow to spherically symmetric perturbations, and (2) a simplified statistical-equilibrium analysis of the relevant ions of carbon, nitrogen, and oxygen using approximate atomic data with the dual objective of improving the line force calculation and estimating the line blanketing due to the expanding envelope.

It is our pleasure to acknowledge the helpful discussions we have had and the assistance we have received from D. G. Hummer and D. Mihalas, whom we also wish to thank for supplying copies of their manuscripts before publication. The seed of the stellar wind theory was planted in conversations of one of us (J. I. C.) with L. H. Auer and D. J. Van Blerkom; their critical comments were very helpful. P. S. Conti and B. E. Bohannan supplied a great deal of advice on how to make comparisons with the observed line spectra.

This work was supported by the National Science Foundation under grant GP-36111 to the University of Colorado.

REFERENCES

Aller, L. H., Faulkner, D. J., and Norton, R. H. 1966, *Ap. J.*, **144**, 1073.
Auer, L. H., and Mihalas, D. 1969, *Ap. J.*, **156**, 157.
Brandt, J. C. 1970, *Introduction to the Solar Wind* (San Francisco: Freeman).
Brandt, J. C., Stecher, T. P., Crawford, D. L., and Maran, S. P. 1971, *Ap. J. (Letters)*, **163**, L99.
Castor, J. I. 1970, *M.N.R.A.S.*, **149**, 111.
———. 1974*a*, submitted to *M.N.R.A.S.* (Paper I).
———. 1974*b*, *Ap. J.*, **189**, 273.
———. 1974*c*, in preparation.
Castor, J. I., and Van Blerkom, D. J. 1970, *Ap. J.*, **161**, 485.
Cayrel, R. 1963, *Compt. Rend.*, **257**, 3309.
Chandrasekhar, S. 1934, *M.N.R.A.S.*, **94**, 522.
Conti, P. S. 1974, *Ap. J.*, **187**, 539.
Conti, P. S., and Leep, E. M. 1974, *Ap. J.*, in press.
Davis, J., Morton, D. C., Allen, L. R., and Hanbury Brown, R. 1970, *M.N.R.A.S.*, **150**, 45.
Hayes, D. S. 1970, *Ap. J.*, **159**, 165.
Heap, S. R. 1972, *Ap. Letters*, **10**, 49.
Hickok, F. R., and Morton, D. C. 1968, *Ap. J.*, **152**, 203.
Johnson, H. L. 1965, *Ap. J.*, **141**, 923.
Lucy, L. B., and Solomon, P. 1970, *Ap. J.*, **159**, 879.
Mihalas, D. 1972, *Non-LTE Model Atmospheres for B and O Stars* (NCAR Technical Note TN-STR/76).
———. 1974, Helen B. Warner Prize Lecture, presented at the 142d meeting of the AAS held at Lincoln, Nebraska, 1974 March 27.

Mihalas, D., and Hummer, D. G. 1974*a*, *Ap. J.* (*Letters*), **189**, L39.
———. 1974*b*, *Ap. J.*, in press.
Mihalas, D., and Lockwood, G. W. 1972, *Ap. J.*, **175**, 757.
Moore, C. E. 1949, *Atomic Energy Levels*, Vol. **1** (*NBS Circ.*, No. 467).
Morton, D. C. 1967, *Ap. J.*, **150**, 535.
Oke, J. B., and Schild, R. E. 1970, *Ap. J.*, **161**, 1015.
Parker, E. N. 1960, *Ap. J.*, **132**, 821.
Stothers, R. 1966, *Ap. J.*, **144**, 959.
Van Blerkom, D. J. 1973, in *Wolf-Rayet and High Temperature Stars*, ed. Bappu and Sahade (Dordrecht: Reidel).

DAVID C. ABBOTT, JOHN I. CASTOR, and RICHARD I. KLEIN: Joint Institute for Laboratory Astrophysics, University of Colorado, Boulder, CO 80302